29th Congress of the International Council
of the Aeronautical Sciences
St. Petersburg, Russia; September 7-12, 2014

HYDRAULIC SYSTEM NOISE REDUCTION BY A COMBINED CONSIDERATION OF FLUID BORNE NOISE AND STRUCTURE BORNE NOISE

Arne Waitschat*, Valérie Pommier-Budinger, Frank Thielecke***

***Hamburg University of Technology, Institute of Aircraft Systems Engineering, Germany**
**** Université de Toulouse, Institut Supérieur de l'Aéronautique et de l'Espace, France**

Keywords: *Hydraulic Noise, Fluid Borne Noise, Structure Borne Noise, Fluid Structure Interaction*

Abstract

A design method is proposed to reduce noise of (aerospace) hydraulic systems. It is based on an accurate model, comprising of fluid-structure interaction. The method aims to keep required system modifications to a minimum by combined tuning of type & location, of existing (a) passive hydraulic silencers and (b) mech. pipe clamps.

1 Introduction

As aircraft engines have been engineered to run quieter in recent years, noise from other aircraft systems is starting to become an issue that can no longer be overlooked. Among these systems, the hydraulic systems produce noise whose main sources are the piston pumps [1], Fig. 1.

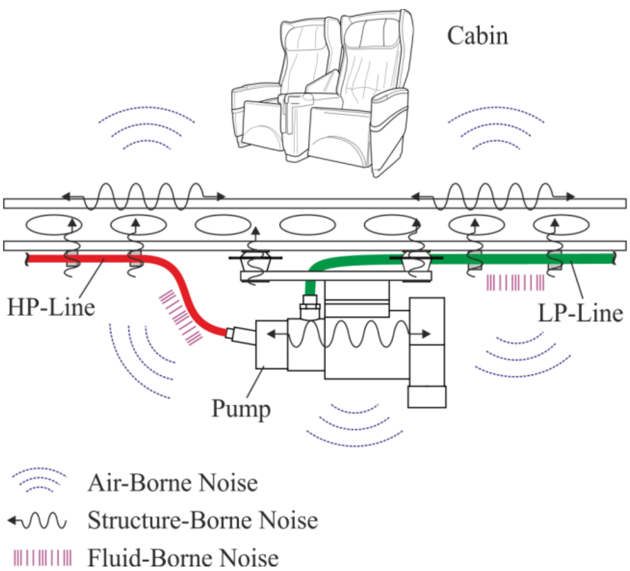

Fig.1. Hydraulic pump noise transmission paths on an aircraft acc. to [1]

Pumps mainly generate fluid-borne noise (FBN) that propagates downstream the system and causes structure-borne noise (SBN) that itself generates air-borne noise (ABN), Fig. 2. In principal, the noise can be tackled at any stage and will reduce noise at all stages below that point [2]. The scope is to decrease vibrations and sound emissions. That means to an increase of component durability and passenger comfort.

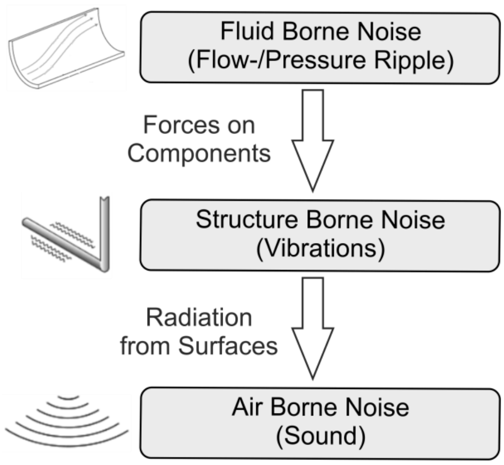

Fig.2. Noise stages (energy level decreasing top to bottom) in terms of hydraulic systems acc. to [2]

FBN takes the form of fluid flow ripple and pressure ripple. It is transmitted through the hydraulic pipes. SBN takes the form of structural force ripple and velocity ripple and is transmitted through pipes and mounts. In terms of hydraulic system noise analysis the FBN stage is generally considered only. In our study, the focus is on FBN plus SBN. This is mainly due to two aspects: First, the aircraft lightweight structure is more sensitive to FBN than many other industrial environments. Second, the typical aerospace constraints – like the need for low equipment size, weight (due to overall A/C performance) & complexity (due to reliability, certification, etc.) – do not allow for radical changes in the design of (in-service) systems. Therefore, solutions with minor hardware adjustments are preferred. Thus we propose a method aiming towards the optimal choice (combined tuning) of type and location of (a) hyd. silencers and (b) mechanical pipe clamps.

The proposed design method is a model-based method. There are a few commercial software packages available to study noise phenomena along hydraulic lines, e.g. Prasp (Univ. of Bath, UK) and DSHplus (Fluidon GmbH, Germany). They allow for FBN prediction; in frequency domain, or in time domain, respectively. Tackling noise at both stages, FBN and SBN, implies taking into account the fluid-structure interaction (FSI) which is not featured in commercial software for the desired noise analysis application yet. Thus, there is a need to extend the existing tools or to develop a new toolbox including FSI. The aircraft industry can be seen as a driver for such an approach, due to the above mentioned particular requirements.

For hydraulic systems, FSI concerns fluid-filled pipes. Basic linear equations governing wave coupling in pipes conveying fluid have been established in several works, e.g. by Wiggert et al. (1987) [3], Brown and Tentarelli (1988) [4], Païdoussis, (1993) [5], de Jong (1994) [6], Tijsseling (1996) [7], Kwong and Edge (1996) [8]. Fundamental work on the optimization of clamp locations was done by Kwong and Edge 1998 [9]. More recent works deal with the nonlinear dynamics of pipes conveying fluid, see e.g. Xu and Yang (2004) [10]. Ibrahim [11] gave a detailed review until 2010. Beyond that, studies on multi-branched pipelines have been done by Jiao et al. (2014) [12], considering complex constraints and boundary conditions.

Using the work of Kwong and Edge (1996) [8] as starting point, a program code has been written to model the combined FBN and SBN behavior, initially for systems of simple straight line elements in series. According to that, the program code first consisted of four differential equations, coupling the fluid pressure/ flow ripple with the axial force/ velocity ripple in the pipes. We extended this work and a work on the optimization of clamp locations – Kwong and Edge (1998) [9] – by adding impedance models of different clamp types, particularly clamps that provide vibrational damping. The program code implementation is based on the transfer matrix technique and allows for studying the combined effect of hydraulic silencers and mechanical pipe clamps.

The paper shows the implemented methodology and simulation results for the mentioned straight in-line element arrangement. Measurements are given that confirm the simulation results.

2 Modeling of Hydraulic System Noise including Fluid Structure Interaction

For FBN simulations on system level a lumped parameter model (LPM) or a 1D–distributed parameter model (DPM) – both using electric-hydraulic analogies – are often applied in oil hydraulics for laminar flow conditions [2]. This can be done in time or in frequency domain.

In terms of FSI, the transfer matrix of each line element increases in size from 2x2 for pressure & flow ripple only, over 4x4, if axial structural forces & velocity are added (here), up to 14x14, if all the structural excitations are introduced. Therefore, the frequency domain is preferred for practical application of FSI, in order to keep simulation time and hardware efforts moderate.

Fluid compressibility, fluid column inertia and resistance to flow are usually represented using the electrical analogies of capacitors, inductors and resistors. If used with sinusoidal potentials (ripples) they become frequency depended impedances. This is also known as impedance modeling technic [2]. The hydraulic impedance represents simply speaking the relation between pressure and flow ripple. Analog, mechanical impedances describe a ratio between force and velocity ripple. Main models are shown below.

2.1 Hydraulic Pump Model

The hydraulic piston pump represents the main noise source. Due to its discrete number of pistons, it generates flow ripple that cause pressure ripple. The pump is usually modeled by a source flow ripple and internal impedance. For both, particular measurements on a dedicated FBN test rig are recommended. The determination of the two pump properties is described e.g. in the ISO 10767 standard (1996, Secondary Source Method) or by Kojima (1992 and 2000, Two pressures/ Two Systems Method) [13, 14]. These properties can also be approximated by physical models. Recently, Baum et al. (2014) [15] introduced a hybrid pump model using both, measured data and an adapted physical model.

In our case no hybrid model but the measured flow ripple of the particular pump were applied as input to the simulation model. The reader is referred to the study case in section 4, where a plot of the input flow ripple is shown along with the rest of the test arrangement and settings.

2.2 Fluid-filled Pipe Model

The pipe represents the main noise transmission path for FBN plus SBN and is of major interest within this study (FSI). The linear basic equations for the complete description of fluid-wave structural coupling in fluid- filled pipes were first given by Wiggert et al. (1987) [3]. They established a set of 14 differential equations including all longitudinal, flexural and torsional movements and flow transients of the pipes. Brown and Tentarelli (1988) [4] modified the equations to take into account of ovalization effects in pipe bends. Kwong and Edge (1996) [8] added a shear coefficient and a frequency-dependent viscosity coefficient.

Our study is limited to the phenomena in axial pipe direction (along z-axes). These consist of the axial stress and the structural velocity along z, and the fluid pressure and flow. The aim is to study the influence of pipe clamps. We consider the four differential equations, respectively [8]:

$$\frac{\partial F_z}{\partial z} + \rho_p \omega^2 A_p u_z - \frac{\lambda_f}{1-\lambda_f} \rho_f \omega^2 A_f u_f = 0 \quad (1)$$

$$(1-\lambda_f)\frac{\partial P}{\partial z} - \rho_f \omega^2 u_f = 0 \quad (2)$$

$$F_z - \frac{A_p \nu D_{int}}{2 t_p} P - A_p E \frac{\partial u_z}{\partial z} = 0 \quad (3)$$

$$P - 2\nu B_{eff} \frac{\partial u_z}{\partial z} + B_{eff} \frac{\partial u_f}{\partial z} = 0 \quad (4)$$

Herein B_{eff} is the effective tangent bulk modulus, represented by the following equation:

$$B_{eff} = \frac{B}{1 + (1-\nu^2)\frac{B D_{int} E}{t_p}} \quad (5)$$

Furthermore, λ_f denotes a friction factor between fluid and pipe wall, approximated with:

$$\lambda_f \approx \frac{4}{D_{int}} \sqrt{\frac{i\vartheta}{\omega}} \quad (6)$$

The used sign conventions are given in Fig.3.

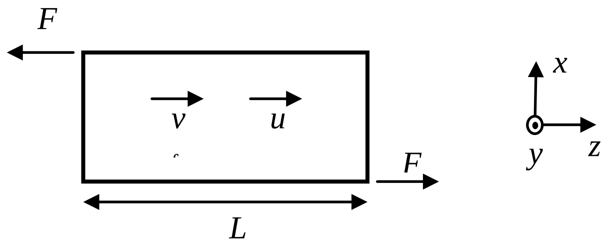

Fig.3. Sign conventions for a pipe element

Describing the fluid cross-sectional area A_f by

$$A_f = \frac{\pi D_{int}^2}{4} \quad (7)$$

And the pipe cross-sectional area A_p with

$$A_p = \frac{\pi (D_{out}^2 - D_{int}^2)}{4} \quad (8)$$

we can rewrite the equations as follows:

$$\frac{\partial P}{\partial z} = \frac{\rho_f \omega^2}{(1-\lambda_f)} u_f \quad (9)$$

$$\frac{\partial F_Z}{\partial z} = -\rho_p \omega^2 A_p u_Z + \frac{\lambda_f}{1-\lambda_f} \rho_f \omega^2 A_f u_f \quad (10)$$

$$\frac{\partial u_f}{\partial z} = -\left(\frac{1}{B_{eff}} + \frac{\nu^2 D_{int}}{t_p E}\right) P + \frac{2\nu}{A_p E} F_z \qquad (11)$$

$$\frac{\partial u_z}{\partial z} = \frac{1}{A_p E} F_z - \frac{\nu D_{int}}{2 t_p E} P \qquad (12)$$

Let us consider the following state vector:

$$X = [P \quad F_z \quad u_f \quad u_z]^t \qquad (13)$$

Then the set of eq. (9) to (12) can be written as:

$$\frac{\partial \dot{X}}{\partial z} = S_X X \qquad (14)$$

With the 4x4 transfer matrix of a considered element of the hydraulic line:

$$S_X = \begin{bmatrix} 0 & 0 & \frac{\rho_f \omega^2}{(1-\lambda_f)} & 0 \\ 0 & 0 & \frac{\lambda_f}{1-\lambda_f} \rho_f \omega^2 A_f & -\rho_p \omega^2 A_p \\ -\left(\frac{1}{B_{eff}} + \frac{\nu^2 D_{int}}{t_p E}\right) & \frac{2\nu}{A_p E} & 0 & 0 \\ -\frac{\nu D_{int}}{2 t_p E} & \frac{1}{A_p E} & 0 & 0 \end{bmatrix} \qquad (15)$$

The transfer matrix of a pipe of length L is then given by:

$$S_{tX} = e^{S_X L} \qquad (16)$$

Using the matrix transfer S_{tX} it is possible to express the output variables of the pipe as functions of the input variables:

$$[P_2 \quad F_{z_2} \quad u_{f_2} \quad u_{z2}]^t = S_{tX} [P_1 \quad F_{z_1} \quad u_{f_1} \quad u_{z1}] \qquad (17)$$

Accounting for cross sectional changes

The set of equations (9) to (12) would have an issue in case of series pipe systems with changes in cross-sectional area. There would be no continuity of the displacements when the sections are changing. So, as proposed in Li et al. (2004) [16], instead of considering the displacements as state variables, we consider the velocities. The new state vector is thus:

$$Y = [P \quad F_z \quad v_f \quad v_z]^t \qquad (18)$$

It verifies the following equation:

$$\frac{\partial \dot{Y}}{\partial z} = S_Y Y \qquad (19)$$

with

$$S_Y = \begin{bmatrix} 0 & 0 & \frac{\rho_f \omega^2}{(1-\lambda_f)} & 0 \\ 0 & 0 & \frac{\lambda_f}{1-\lambda_f} \rho_f \omega^2 A_f & -\rho_p \omega^2 A_p \\ -\left(\frac{1}{B_{eff}} + \frac{\nu^2 D_{int}}{t_p E}\right) & \frac{2\nu}{A_p E} & 0 & 0 \\ -\frac{\nu D_{int}}{2 t_p E} & \frac{1}{A_p E} & 0 & 0 \end{bmatrix} \qquad (20)$$

Normalization of state variables

Computing the matrix exponential $S_{tY} = e^{S_Y L}$ may lead to numerical problems if the variables are not normalized [8]. Thus the scaling factors of Table 1 below are used for a normalized representation of the state variables such that:

$$P = k_P \hat{P}, \qquad v_f = k_P \widehat{v_f}, \qquad F_z = k_P \widehat{F_z}, \qquad v_z = k_P \widehat{v_z} \qquad (21)$$

Description	Normalized state variable	Scaling factors
Fluid-pressure	$\hat{P}$	$k_P = P_O$
Fluid-velocity	$\widehat{v_f}$	$k_{v_f} = \frac{P_O}{\rho_f c^2}$
Structural-force	$\widehat{F_z}$	$k_{F_z} = P_O A_f$
Structural-velocity	$\widehat{v_z}$	$k_{v_z} = \frac{P_O}{E A_p}$

Tab.1. Scaling factors for normalized state variables

The new state vector is thus:

$$\hat{Y} = [\hat{P} \quad \widehat{F_z} \quad \hat{v}_f \quad \hat{v}_z]^t \qquad (22)$$

It verifies the following equation:

$$\frac{\partial \widehat{Y}}{\partial z} = \hat{S}_Y \hat{Y} \qquad (23)$$

With final form of the transfer matrix:

$$\hat{S}_Y = \begin{bmatrix} 0 & 0 & -\frac{\rho_f \omega}{(1-\lambda_f)} i \frac{k_{v_f}}{k_P} & 0 \\ 0 & 0 & -A_f \frac{\lambda_f}{(1-\lambda_f)} \rho_f \omega i \frac{k_{v_f}}{k_{F_Z}} & \rho_p A_p \omega i \frac{k_{v_Z}}{k_{F_Z}} \\ -\left(\frac{1}{B_{eff}} + \frac{\nu^2 D_{int}}{t_p E}\right) \omega i \frac{k_P}{k_{v_f}} & \frac{2\nu}{A_p E} \omega i \frac{k_{F_Z}}{k_{v_f}} & 0 & 0 \\ -\frac{\nu D_{int}}{2 t_p E} \omega i \frac{k_P}{k_{v_Z}} & \frac{1}{A_p E} \omega i \frac{k_{F_Z}}{k_{v_Z}} & 0 & 0 \end{bmatrix} \quad (24)$$

2.3 Line-Terminator Model

Multiple termination options for the hydraulic line are available in commercial FBN software packages. These are e.g. closed ends, open ends, restrictor valves and anechoic (reflection-less termination), see [17]. In our case, an anechoic termination was modeled using a combination of a 20m hose, a resistance and an open end to keep the model closest in meaning to the physical test rig. The 20m hose was chosen to represent the low reflection characteristics of the test rig. The resistance was chosen to represent the load valve utilized and the open end is supposed to model the return line to the reservoir. In an ideal case, the pressure is null for an open end. Concerning the mechanical behavior, we also assume that:

$$F_Z = 0 \text{ and } u_Z = 0 \quad (25)$$

A test rig diagram and a screenshot of the model are both given in the appendix for comparison.

2.4 Mechanical Clamp Model

Two kinds of clamps will be investigated in this paper and are further described below:

- Clamps in Polypropylene, Fig. 4.
- Clamps in Polypropylene with an Elastomer part, Fig.5.

We considered a simple linear model of the pipe clamps by the mechanical impedance Z_{clamp}:

$$Z_{clamp} = K'_c + iK''_c \quad (26)$$

Where:

- K'_c is the axial stiffness.
- K''_c represents the loss produced by the clamp and is assumed to be equal to

$$K''_c = tan(\delta)K'_c \quad (27)$$

with $tan\delta$ as the loss factor that depends on the chosen clamp materials, see Table 2.

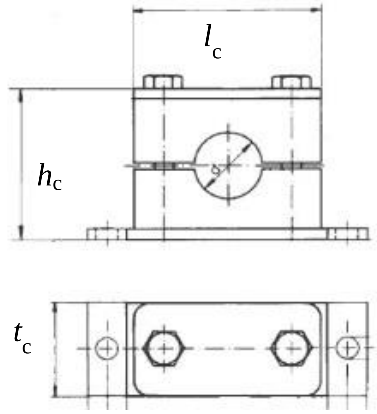

Fig. 4. Clamp in polypropylene

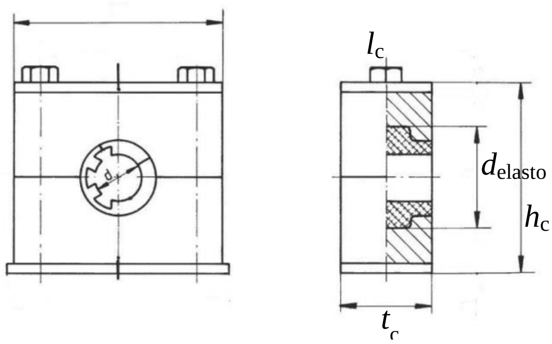

Fig.5. Clamp in polypropylene with elastomer

Loss Factor $tan\delta$	Material
10^0 and more	Elastomer
10^{-2}	Polypropylene
10^{-3}	Steel

Tab.2. Loss factor for different materials

The required axial stiffness is measured by a compression test in a traction machine for a pipe clamp of an inner diameter of 42mm, Fig.6. A regression in the linear part of the curve "Force versus Displacement", Fig. 7 and Fig. 8, enables to evaluate the axial stiffness of the pipe clamp:

- Clamps in Polypropylene: K'_c = 1.8e7 N/m
- Clamps in Polypropylene plus Elastomer: K'_c = 2.5e6 N/m

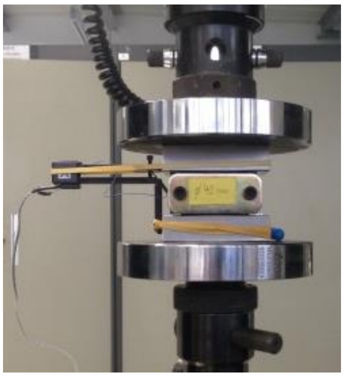

Fig.6. Axial stiffness test of a hydraulic pipe clamp

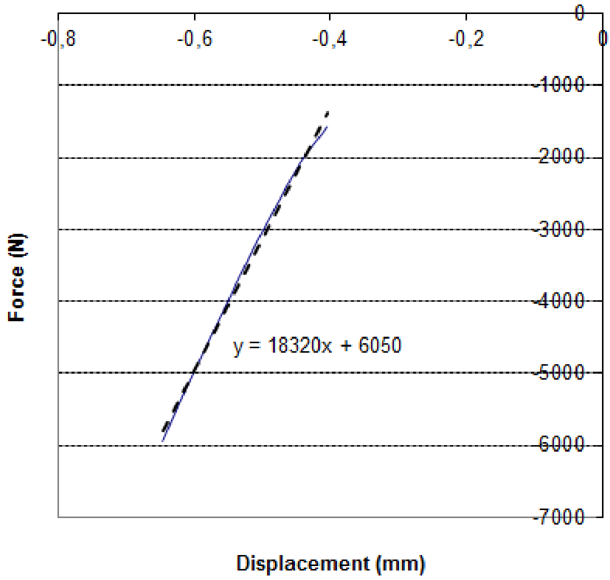

Fig.7. Axial stiffness test results for a hydraulic clamp in polyproprylene **without** elastomer

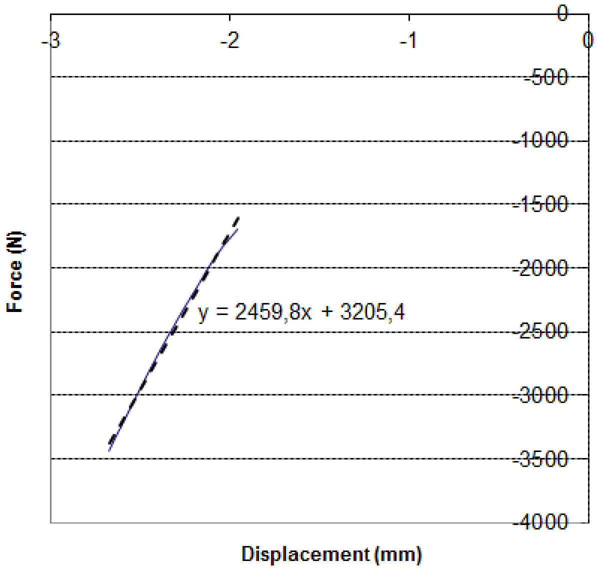

Fig.8. Axial stiffness test results for hydraulic clamp in Polypropylene **with** elastomer

3 Computation Method for Hydraulic Noise including Fluid Structure Interaction

The procedure to compute the fluid flow/ pressure ripple and the axial structural force/ velocity ripple in case of a straight hydraulic system with no intersections is given below:

Step 1: Compute the characteristics in each pipe (speed of sound, flow cross-sectional area, frictional factor).
Step 2: Compute the normalization factors.
Step 3: Write the normalized matrix $\hat{S}_Y$ and compute the pipe transfer matrix $S_{t\hat{Y}} = e^{S_{\hat{Y}}L} = [S_{t\hat{Y}}(i,j)]$ that corresponds to the vector $\hat{Y} = [\hat{P} \quad \hat{F}_Z \quad \hat{v}_f \quad \hat{v}_z]^t$.
Step 4: For each pipe: Compute the pipe transfer matrix T_k that corresponds to the vector $W = [\ P, F_Z, Q, v_z]$.

$$T_k = \begin{bmatrix} S_{t\hat{Y}}(1,1) & S_{t\hat{Y}}(1,2)\frac{k_P}{k_{F_z}} & S_{t\hat{Y}}(1,3)\frac{k_P}{A_f k_{v_f}} & S_{t\hat{Y}}(1,4)\frac{k_P}{k_{v_z}} \\ S_{t\hat{Y}}(2,1)\frac{k_{F_z}}{k_P} & S_{t\hat{Y}}(2,2) & S_{t\hat{Y}}(2,3)\frac{k_{F_z}}{A_f k_{v_f}} & S_{t\hat{Y}}(2,4)\frac{k_{F_z}}{k_{v_z}} \\ S_{t\hat{Y}}(3,1)\frac{A_f k_{v_f}}{k_P} & S_{t\hat{Y}}(3,2)\frac{A_f k_{v_f}}{k_{F_z}} & S_{t\hat{Y}}(3,3) & S_{t\hat{Y}}(3,4)\frac{A_f k_{v_f}}{k_{v_z}} \\ S_{t\hat{Y}}(4,1)\frac{k_{v_z}}{k_P} & S_{t\hat{Y}}(4,1)\frac{k_{v_z}}{k_{F_z}} & S_{t\hat{Y}}(4,3)\frac{k_{v_z}}{A_f k_{v_f}} & S_{t\hat{Y}}(4,4) \end{bmatrix} \quad (28)$$

Step 5: Compute the boundary conditions at both ends of the system. For a hydraulic system with n series pipes, the transfer matrix of the system T_{system} is the product of the transfer matrices of each pipe T_k:

$$T_{system} = \prod_{k=1}^{n} T_k \tag{29}$$

Thus a set of equations linking the boundaries conditions W_1 and W_{n+1}, respectively at the beginning and at the end of the pipe system, can be written as:

$$W_{n+1} = T_{system}\, W_1 \tag{30}$$

Step 6:
In order to incorporate the clamps in the hydraulic system model by using the transfer matrix technique, we implement the method described in the work of Lin and Donaldson (1969) [18]. Consider a clamp after pipe element r. Then the model of the hydraulic circuit is written:

$$\begin{aligned} W_2 &= T_1\, W_1 \\ W_3 &= T_2\, W_2 \\ &\vdots \\ W_{r+1} &= T_r\, W_r \\ W_{r+2} &= T_c\, W_{r+1} \\ W_{r+3} &= T_r\, W_{r+2} \\ &\vdots \\ W_{n+1} &= T_{n-1}\, W_n \\ W_{n+2} &= T_n\, W_{n+1} \end{aligned} \tag{31}$$

Here T_c is the clamp transfer matrix defined by:

$$T_c = \begin{bmatrix} 1 & 0 & 0 & 0 \\ 0 & 1 & 0 & 0 \\ 0 & 0 & 1 & 0 \\ 0 & 0 & 0 & 1 - Z_c \end{bmatrix} \tag{32}$$

Step 7: There are known and unknown boundary conditions at both ends of the circuit. By solving the equations (33), all boundary conditions at both ends can be determined.

Step 8: Compute the variables $W_i = [\,P_i, F_{Z_i}, Q_i, v_{z_i}]$ at each extremity i (each node) of the pipe line by using the following set of equations (33).

$$\begin{aligned} W_2 &= T_1\, W_1 \\ W_3 &= T_2\, W_2 \\ &\vdots \\ W_n &= T_{n-1}\, W_{n-1} \\ W_{n+1} &= T_n\, W_n \end{aligned} \tag{33}$$

4 Design for quieter Hydraulic Systems

4.1 Strategy

The method to design quieter hydraulic systems is proposed in Fig. 9. The main steps are:
Step 1: Choice of type and location of hydraulic silencer to reduce the fluid-borne noise.
Step 2: Choice of type and location of mechanical pipe clamps to reduce the remaining structure-borne noise.
The method is an iterative method depending on the validation of the requirements.

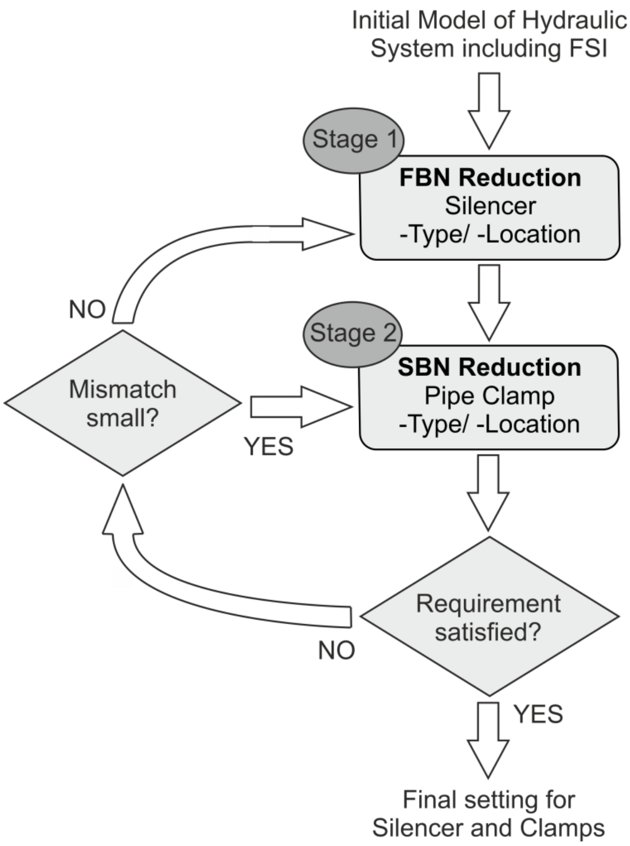

Fig.9. Strategy to design quieter hydraulic systems by a combined consideration of fluid-borne noise (FBN) and structure-borne noise (SBN)

4.2 Study case

The study case compares simulation results with measurement results for a given reference test setting at a noise test rig at Hamburg University of Technology. Since the general modelling was already described in section 2 and 3, a brief introduction of the test setting is given below. Detailed diagrams of the compared setting and simulation model are shown in the appendix.

The study case is dealing with hydraulic noise that is induced by a typical aircraft Electrical-Motor Pump and a typical mean system pressure of approximately 200bar. Here, a seven piston-pump was utilized and driven with a shaft speed of 7800 rpm. Therefore, the pump generates flow ripple with high peaks at a shaft frequency of 130 Hz, a piston frequency of 910 Hz and their harmonics, see spectrum in Fig. 10. The design method is applied to decrease FBN and SBN impact due to these flow ripples. The measured pump flow ripple spectrum is taken as input for the simulation model.

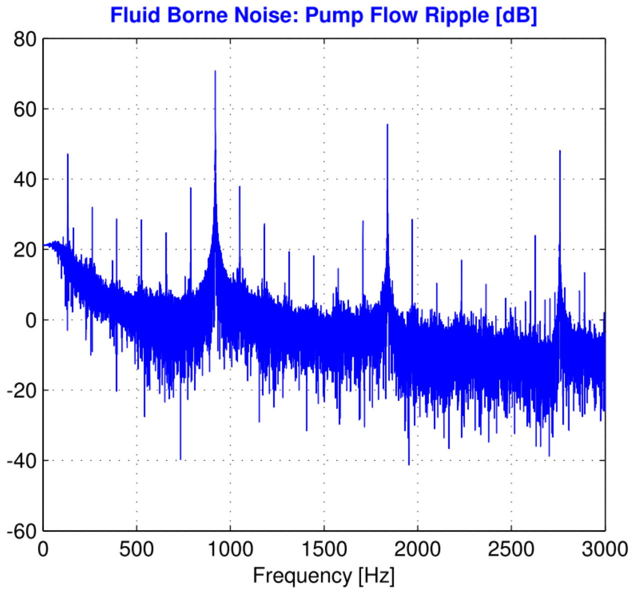

Fig.10. Pump flow ripple taken from measurements

The pump delivers the flow directly through a hydraulic silencer (if applied, see config. 1 to 3) into a straight test pipe equipped with dynamic pressure transducers (for FBN) and acceleration sensors (for SBN). The rear end of the test pipe is connected to a 20m hose that serves as low-reflection line ending for the test pipe. After the hose a load valve block takes place, where the mean flow demand is adjusted by a needle valve to a relatively low flow rate of approx. 5 lpm. Fig. 11 gives an idea auf the main components. Details on the hydraulic diagram can be found in the appendix. The test pipe is mounted with clamps. Those are subject to modifications.

The mentioned hydraulic silencer is chosen to attenuate the fluid born noise on a broad band frequency range over a few piston frequency harmonics of the pump. This will be confirmed by test and simulation, shown on the next pages.

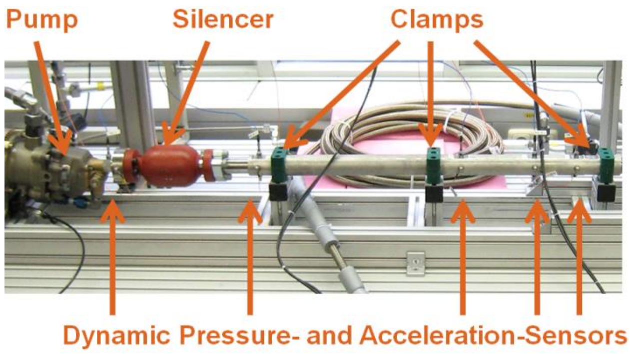

Fig.11. Picture of the main test rig components

The pump flow ripple causes pressure ripple and acceleration ripple that are measured at several positions along the hydraulic line. All the following **plots are given exemplarily for a point along the line btw the second and third clamp** (counting from the left).

The measured acceleration ripples are integrated to velocity ripples in order to allow comparison with simulation results. Furthermore, the velocity ripples and the pressure ripples have to be post-processed with an FFT algorithm, so we can compare them with the frequency domain results of the simulation tool.

4.2.1 Configuration 1: Reference Condition

The first measurements are performed on the hydraulic line without silencer and an initial pipe clamp setting using PP clamps, Fig. 12. This configuration is considered as the reference case. The plots show a good agreement between measurement and simulation (see peak values) and allow validating the simulation tool.

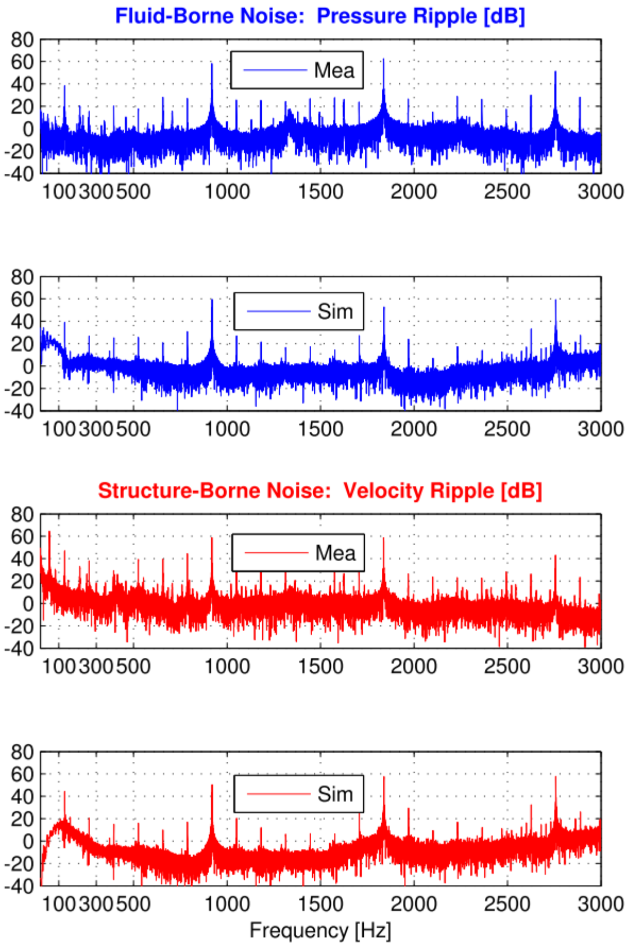

Fig. 12. Noise spectra of system without hydraulic silencer and an initial pipe clamp setting using PP (Reference condition)

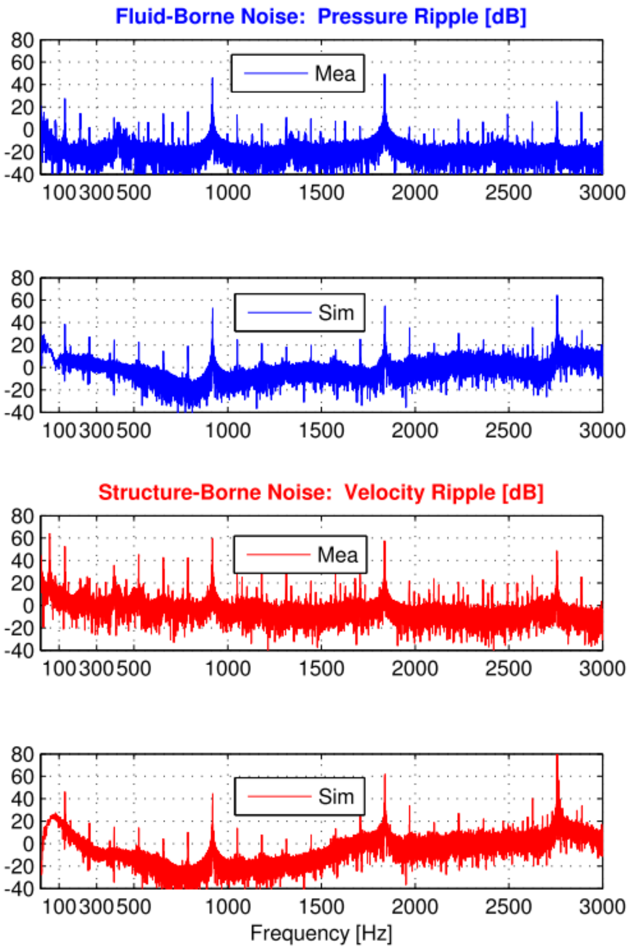

Fig.13. Noise spectra of system **with** hydraulic silencer, but still initial pipe clamp setting using PP

4.2.2 Configuration 2: FBN reduction

For this configuration, a hydraulic silencer was chosen to attenuate the fluid born noise on a broad band frequency range over a few of the piston frequency harmonics of the pump. Both – measurement and simulation – reflect the expected silencer performance, Fig. 13: An FBN Insertion Loss (IL) of 10-20dB compared to the reference condition, Fig. 12. For frequencies higher than ~2500 Hz the effect of the silencer is not clearly visible in case of the simulations. Here the general confidence limits of the impedance modelling technic are reached. As further expected, the SBN is negligibly affected by the hydraulic silencer due to the structural path across the silencer wall. Some higher harmonics even increase. Measurements increase less than simulations, because SBN can also escape along the real pump housing, which was not modeled for simulation.

4.2.3 Configuration 3: SBN reduction

The third configuration aims at studying the influence of the clamps on the SBN reduction, Fig. 14 and 15. Compared to configuration 2, the clamps are modified from PP clamps to PP clamps with elastomer. Results are shown for simulation only, because good accordance to measurements was shown with Fig. 12 and 13.

As expected, the FBN is not affected by the clamps, because FBN has a higher energy level than SBN. However, the introduction of softer clamps (with elastomer) does increase the SBN for the pipe wall, Fig. 14 and 15, which means less energy is transmitted to the local attachment structure (SBN reduction on structure-side). The increase of pipe SBN is more clearly visible in Fig. 15 (peaks amplified up to 20 dB), than in Fig 14. This is because the clamp modifications took place on opposite sides of the ref. point.

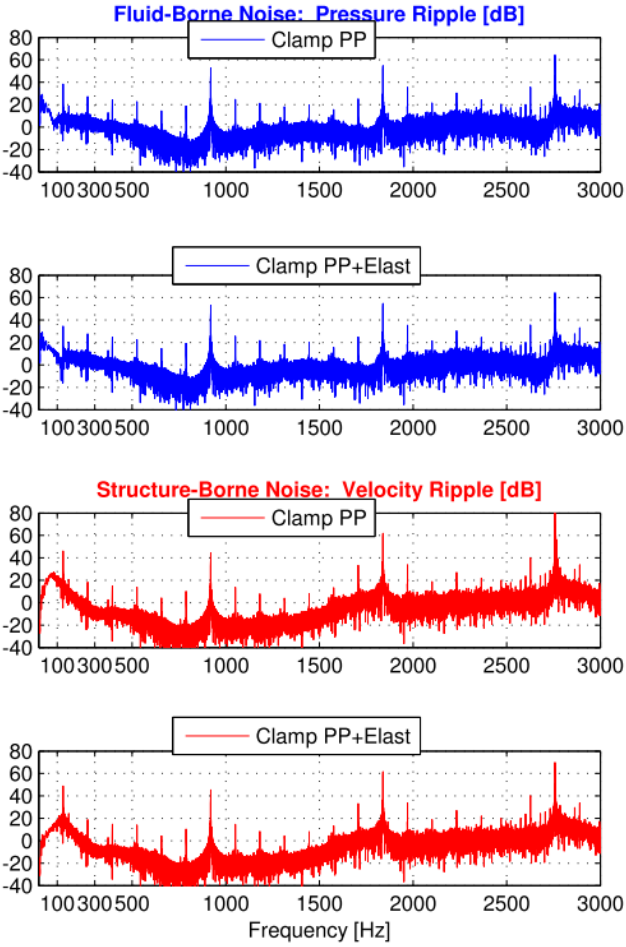

Fig.14. Noise spectra of system **with** hydraulic silencer and **with first** pipe clamp type modified from (PP) to (PP with elastomer)

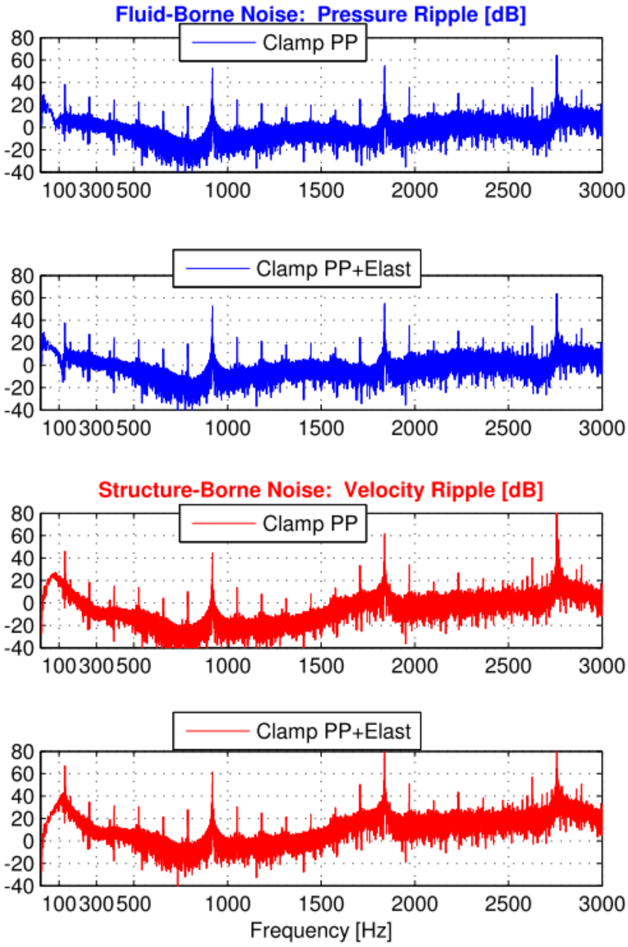

Fig.15. Noise spectra of system **with** hydraulic silencer and **with third** pipe clamp type modified from (PP) to (PP with elastomer)

5. Conclusion

This paper proposes a model-based design methodology for a combined consideration/ reduction of fluid-borne noise (FBN) and structure-borne noise (SBN) of hydraulic systems. This is driven by the restrictive aircraft environment. Here, noise reduction has to be achieved by minimum equipment modifications. Therefore, the methodology comprises of two items:

1) A **computation tool** with fluid-structure interaction (FSI) prediction capabilities. Such a tool was derived and a successful application example was given.

The example was limited to straight lines with no intersections. However, in the meantime the capabilities of the tool were extended with inter-sections and other features. The tool was designed in MATLAB-Simulink/Simscape. It consists of a user defined element library and serves as graphical user interface (GUI).

The mentioned introduction of all FSI-equations in the tool is under development, to allow describing the FSI problem in 3D.

2) An overlaying **design strategy** was introduced that aims to use the tool to optimize type and location of existing hydraulic silencers and mechanical clamps, abort commercial aircrafts.

FBN and SBN treatment are considered in a common and iterative optimization process that is under development.

References

[1] Kohlberg M, Thielecke F, Heise U and Behr R M. *Novel concepts for noise reduction in aircraft hydraulic systems*. Deutscher Luft- und Raumfahrt Kongress (DLRK), Bremen, Germany, Vol. 60, paper number 241318, pp 429-436, September 27-29, 2011.

[2] Johnston N and Tilley D. *Noise in Hydraulic Systems.* Course Manuscript, Center for Power Transmission and Motion Control (PTMC), University of Bath, UK, 2013.

[3] Wiggert D C, Hatfield F J and Stuckenbruck S. *Analysis of liquid and structural transients in piping by the method of characteristics*. Journal of Fluids Engineering, Vol. 109, pp. 161-165, 1987.

[4] Brown F T and Tentarelli S C. *Analysis of noise and vibration in complex tubing systems with fluid-wall interaction*. Proceedings of the forty-third national conference on Fluid power, pp. 139-149, 1988.

[5] Païdoussis M P and Li G X. *Pipes Conveying Fluid: A Model Dynamical Problem*. Journal of Fluids and Structures, Vol. 7, Issue 2, pp. 137-204, 1993.

[6] de Jong C A F. *Analysis of pulsations and vibrations in fluid-filled pipe systems*, Ph.D. thesis, TNO Institute of Applied Physics, Delft, 1994.

[7] Tijsseling A S. *Fluid-structure interaction in liquid-filled pipe systems: a review*, Journal of Fluids and Structures, Vol. 10, pp. 109-146, 1996.

[8] Kwong A H M and Edge K A. *Structure-borne noise prediction in liquid-conveying pipe systems*. Proceedings of the Institution of Mechanical Engineers, Part I: Journal of Systems and Control Engineering, pp. 189-200, 1996.

[9] Kwong A H M and Edge K A. *A method to reduce noise in hydraulic systems by optimizing pipe clamp locations*. Proceedings of the Institution of Mechanical Engineers, Part I: Journal of Systems and Control Engineering, pp. 212-267, 1998.

[10] Xu J and Yang Q B. *Recent development on models and nonlinear dynamics of pipes conveying fluid*. Adv. in Mechanics, Vol. 34(2), pp. 182-194, 2004

[11] Ibrahim R A. *Overview of Mechanics of Pipes Conveying Fluids—Part I: Fundamental Studies*. Journal of Pressure Vessel Technology, Vol. 132, 034001, 2010.

[12] Jiao Z, Xu Y, Johnston N and Plummer A R. *Frequency modelling and solution of fluid-structure interaction in complex pipelines.* Journal of Sound and Vibration, Vol. 333, pp. 2800-2822, 2014.

[13] Kojima E. *A New Method for the Experimental Determination of Pump Fluid-Borne Noise Characteristics*. Proceedings of the 5th Bath International Fluid Power Workshop, Circuit, Component and System Design, pp. 111-135, 1992.

[14] Kojima E, Yu J and Ichiyanagi T. *Experimental Determining and Theoretical Predicting of Source Flow Ripple Generated by Fluid Power Piston Pumps*. SAE Technical Paper Series, No. 2000-01-2617, 2000.

[15] Baum H, Becker K and Faßbender A. *Hybrid Pump Model for 1D Hydraulic System Simulation*. International Fluid Power Conference (IFK), Aachen, Germany, Vol. 9, pp.38-49, March 24-26, 2014.

[16] Li Q S, Yang K and Zhang L. *Longitudinal vibration analysis of multi-span liquid-filled pipelines with rigid constraints*. Journal of Sound and Vibration, Vol. 273, pp. 125-147, 2004.

[17] N.N. *Prasp – Pressure Ripple Analysis Software Package*, User Guide and Reference Manual, Version 5.01.00, University of Bath, UK, 2007.

[18] Lin Y K and Donaldson B K. *A brief survey of transfer matrix techniques with special reference to the analysis of aircraft panels*. Journal of Sound and Vibration, Vol. 10, pp. 103-143, 1969.

Notation

A_c	Clamp cross-sectional area	m²
A_p	Pipe cross-sectional area	m²
A_f	Fluid cross-sectional area	m²
B	Fluid bulk modulus	m
B_{eff}	Effective bulk modulus	m
c	Speed of sound	m/s
D_{int}	Pipe inner diameter	m
D_{int}	Pipe inner diameter	m
$D_{c_{int}}$	Clamp inner diameter	m
$D_{c_{out}}$	Clamp outer diameter	m
E	Pipe Young’s modulus	Pa
F_z	Axial Force	N
G_c	Shear modulus of the clamp	Pa
h_c	Clamp height	m
L	Pipe length	m
l_c	Clamp length	m
P	Fluid pressure	Pa
P_0	Fluid pressure (static)	Pa
Q	Fluid flow	m^3/s
t_c	Clamp thickness	m
t_p	Pipe thickness	m
u_f	Fluid displacement	m
u_z	Str. displacement along z	m
v_f	Fluid velocity	m/s
v_z	Structural velocity along z	m/s
Z_c	Clamp impedance	
λ_f	Frictional factor	
ϑ	Fluid kinematic viscosity	m^2/s
ν	Poisson’s ratio	
ρ_f	Fluid density	Kg/m^3
ρ_p	Pipe density	Kg/m^3
ω	Angular frequency	(rad/s)

Contact Author Email Address

Arne Waitschat (TUHH):
arne.waitschat@tuhh.de
Tel: +4940428788229

Valérie Budinger (ISAE):
valerie.budinger@isae.fr
Tel: +33561339120

Copyright Statement

Appendix

Details on the noise test rig setting, Fig.16, and the according simulation model, Fig.17, are shown below:

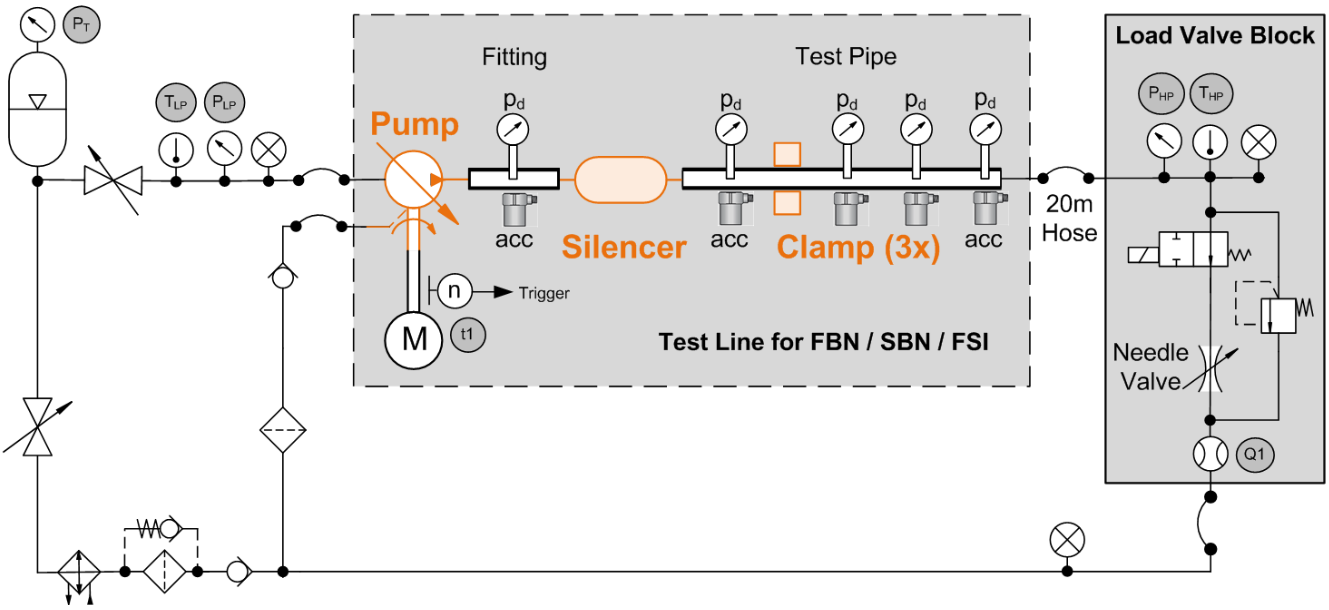

Fig.16. Diagram of the used noise test rig setting for the mentioned study case

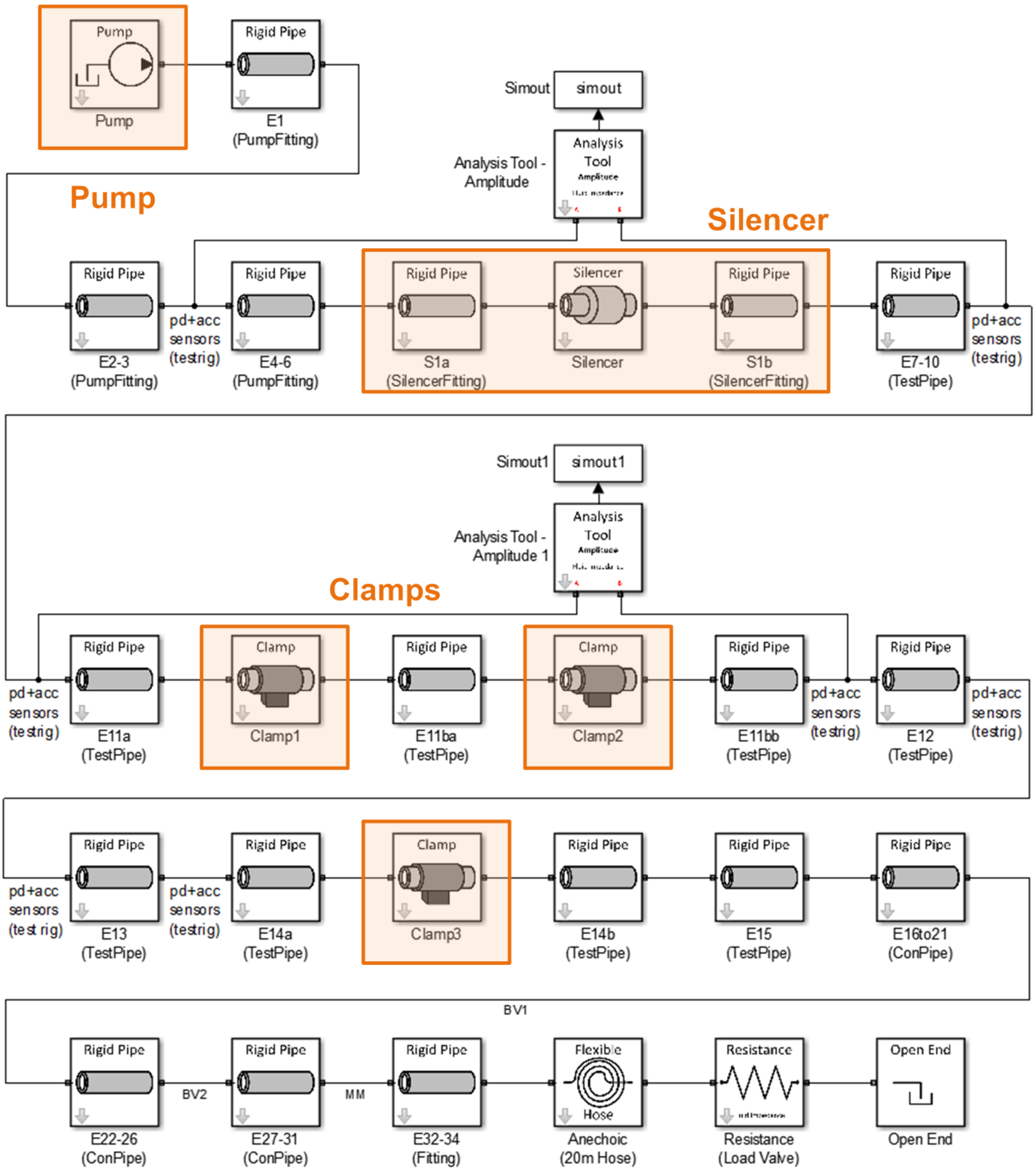

Fig.17. Screenshot of the used noise simulation model for the mentioned study case
The model was built with an in-house FBN/SBN/FSI-Tool/Library
designed in the MATLAB-Simulink/Simscape environment